# A Prototype Electrical Actuator for Aircraft Flaps

John W. Bennett, Barrie C. Mecrow, *Member, IEEE*, Alan G. Jack, *Member, IEEE*, and David J. Atkinson

***Abstract*—This paper considers the electrical actuation of aircraft wing surfaces, with particular emphasis on flap systems. It discusses existing hydraulic and electrohydraulic systems and proposes an electrical alternative, examining the potential system benefits in terms of increased functionality, maintenance, and life-cycle costs. This paper then progresses to describe a full-scale actuation demonstrator of the flap system, including the high-speed electrical drive, step-down gearbox, and flaps. Detailed descriptions of the fault-tolerant motor, power electronics, control architecture, and position sensor systems are given, along with a range of test results, demonstrating the system in operation.**

***Index Terms*—Actuator, aerospace drive, fault tolerance, permanent magnets, redundancy.**

## I. Introduction

THIS work is driven by the desire to remove hydraulic actuation from aircraft control surfaces as part of the move toward "more electric" aircraft. Particular attention is focused here on the flap actuation system. The target for this research is future civil aircraft, but the results are equally relevant to military projects. The flaps require considerably less power than fast-acting primary control surfaces, i.e., ailerons, rudder, and elevator, and in terms of safety, it is acceptable to freeze the flaps, provided that symmetry is maintained across the two wing surfaces. Any replacement of the current arrangements must ensure symmetry and meet all existing safety requirements. Life-cycle costs can be reduced by increasing reliability and, therefore, aircraft availability.

The existing arrangement for the actuation of commercial aircraft flaps usually consists of two mechanically summed hydraulic motors driven from two independent hydraulic supplies. The hydraulic supplies are generated from pumps driven by auxiliary gearboxes on the engines. The motors are located within the body of the aircraft and drive the flaps using a mechanism of gearboxes and torque tubes. Although the flaps are mechanically linked to move in unison to guarantee symmetry at all times, the relative position of all flaps is monitored, and the hydraulic system locks all flaps when a small amount of asymmetry occurs. Complete failure of hydraulic power also results in locking of the flap system.

There have been a number of moves toward electric actuation of aircraft surfaces ranging from as early as 1916 [1]. In recent times, there has been a gradual move to electric actuation, as in the flap system of the Boeing 777, featuring a fly-by-wire hydraulic motor as a primary actuation source and an electric drive, coupled via clutch, as a secondary backup [2]. An electromechanical actuator is used for the combined flaps/ailerons (so-called "flaperons") on an F18 fighter in the US EPAD program [3]. Systems have also been flight tested on C130 and C141 military transport aircraft by the Lockheed-Georgia Company [4], [5]. In a purely electromechanical solution, it is harder to incorporate redundancy than in hydraulic solutions, and providing holding force is considerably more difficult than simply closing a valve. This has led to electrohydraulic systems [6], which remove most of the high-pressure hydraulic plumbing.

The research that underpins this paper aims to explore the technical and economic issues associated with electromechanically driven flap systems. It was established in an outline study that useful system gains could be made if the direct mechanical coupling of all of the flap sections (as per current commercial practice) was abandoned. A fully distributed electrical approach to the actuation of flaps aims to replace the central hydraulic motor and drive shafts across the wingspan with an individual actuator for each high-lift surface. This gives greater functionality, but reliability requirements have meant that a fault-tolerant motor and controller are required for each actuator.

Bennett *et al.* [7] discussed the selection of an appropriate fault-tolerant motor/drive topology to achieve the required reliability with the optimum component count and mass. In [8], they discussed the fault-tolerant control methods employed to control this specialist electric drive. A full-scale working flap rig has now been produced, with working fault-tolerant electrical architectures. This paper discusses new material relating to the production and testing of the complete rig, which reproduces actual operating conditions and has enabled full testing of the actuation systems under normal and faulted conditions.

### A. Potential Benefits of Electrical Systems

The electrical system has been designed to reduce overall life-cycle costs while increasing system reliability and functionality. The potential benefits are listed here.

1) Reduced maintenance due to the modular nature of the system. A failed actuator can be removed without the need to dismantle sections of the common driveshaft across the wingspan.
2) Increased functionality since there is individual control of each flap; it is no longer necessary to deploy all flaps at the same rate or to the same angle.

Paper IPCSD-09-012, presented at the 2005 IEEE International Electric Machines and Drives Conference, San Antonio, TX, May 15–18, and approved for publication in the IEEE TRANSACTIONS ON INDUSTRY APPLICATIONS by the Electric Machines Committee of the IEEE Industry Applications Society. Manuscript submitted for review April 1, 2006 and released for publication July 8, 2009. First published March 25, 2010; current version published May 19, 2010. This work was supported by EPSRC, Eaton Aerospace (formerly FR-Hitemp), BAE Systems Rochester, BAE Systems Woodford, and by the U.K. Department of Trade and Industry.

The authors are with the Department of Electrical, Electronic and Computer Engineering, University of Newcastle upon Tyne, Newcastle upon Tyne, NE1 7RU, U.K. (e-mail: john.bennett@ncl.ac.uk; barrie.mecrow@ncl.ac.uk; alan.jack@ncl.ac.uk; dave.atkinson@ncl.ac.uk).

Digital Object Identifier 10.1109/TIA.2010.2046278

0093-9994/$26.00 © 2010 IEEE

Authorized licensed use limited to: Newcastle University. Downloaded on May 21,2010 at 13:17:05 UTC from IEEE Xplore. Restrictions apply.

3) Improved fault detection, as all monitoring is electronic and (can be) transmitted to the pilot.
4) Wear and degradation can be monitored by the control system to enable preemptive fault maintenance. For example, discrepancies between motor position sensors and linear sensors or excessive no-load current could indicate wear and predict a failure.
5) Reduced mass.

However, because the system has more components acting in parallel, it is more complex and therefore requires a level of redundancy and fault tolerance to meet the reliability requirements.

### B. System Specification

A midsized commercial aircraft, with a take-off mass of 180 t, has been chosen for this research. The aircraft has two flaps per wing, with a maximum load per flap of 34 kN $\cdot$ m. Flaps must be extended within a time period of 30 s and retracted within 20 s. Of course, they are normally only deployed at takeoff and landing, so the duty cycle is rather low. The most arduous duty cycle may occur during training or flight test conditions, when an absolute maximum of three cycles every 500 s may be encountered.

When retracted, the flap positions must be synchronized to within 0.25% of their full travel, whereas, at all other positions, they must be within 0.5%. This requirement is essential since it is flight critical: uncontrolled movement of the flaps will be catastrophic and must meet reliability requirements of less than $10^{-9}$ failures per flight hour. This requirement is several orders of magnitude beyond what can be achieved with an electrical actuation system, and so, in the event of a complete failure of the electrical system, power-off friction brakes are used to lock the system and maintain symmetry. It is possible to lock the system by employing a gearbox that will not back-drive, although this limits the design of the gearbox, which now also needs to meet $10^{-9}$ failures per flight hour. In this paper, studies showed that the power-off brake solution was better than the use of the gearbox for this function.

A locked high-lift system is not catastrophic, but it will result in an aborted departure or emergency landing. Consequently, a reduced reliability requirement of $10^{-5}$ failure/h is acceptable, based on trade studies of the economics of aircraft operation (a mean time between failures of 11 years). Conventional motor and power electronic drives still cannot meet this requirement [9], [10], typically having failure rates that are rather more than $10^{-5}$ failure/h; hence, fault tolerance and redundancy must be used in the motor and power electronics to allow the system to run with one fault. A fault-tolerant motor drive system can attain levels of $10^{-7}$ failure/h [11]. Reduced speed of operation is tolerated when faulted, provided that the speed is in the range of 20%–70%, and there are less than $10^{-3}$ occurrence/h.

Ambient conditions are very variable: when flying, there can be ambient temperatures as low as $-40$ °C and, hence, very good cooling by convection. However, the system must also offer full performance with the plane stationary on a runway at an ambient of up to 70 °C.

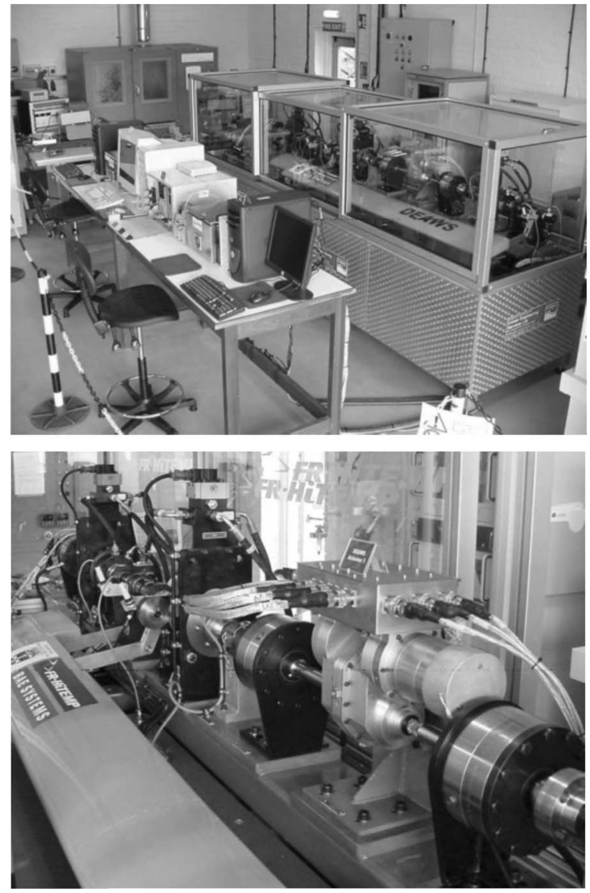

Fig. 1. Full twin flap test rig.

### C. System Architecture

An exceptionally high-load torque at very low velocity is required at the flap surface; hence, it is essential to use a highly geared system. A high-reliability gearbox has been designed and constructed for this purpose, so that the load torque is delivered by an electrical machine rotating at a maximum speed of 10 000 r/min and delivering a maximum output power of 3.5 kW (enough to power a flap of an A320-sized aircraft).

A single electrical drive is used to move each flap. Because the flap is several meters long, it is necessary to drive both ends to prevent the flap from sticking at the undriven end. Consequently, the drive is placed centrally on the flap, with a hard mechanical coupling to each end.

Photographs of the demonstrator rig are shown in Fig. 1, and the overall demonstrator rig is diagrammatically illustrated in Fig. 2. The rig comprises one full flap section and one half-flap section. Each flap is driven by a modular fault-tolerant drive, with overall system control undertaken by a flap control computer. A full description of the overall control and monitoring system is beyond the scope of this paper, but a brief description of the overall scheme will help to set the context for the description of the actuator. The flap control computer sets a flap position command, which is fed to three separate drive modules (A, B, and C in Fig. 2). Each drive module has a conventional position control using nested position, speed, and torque loops. The angle of the flap is measured using multiple linear position sensors, which are separate from and in

Authorized licensed use limited to: Newcastle University. Downloaded on May 21,2010 at 13:17:05 UTC from IEEE Xplore. Restrictions apply.

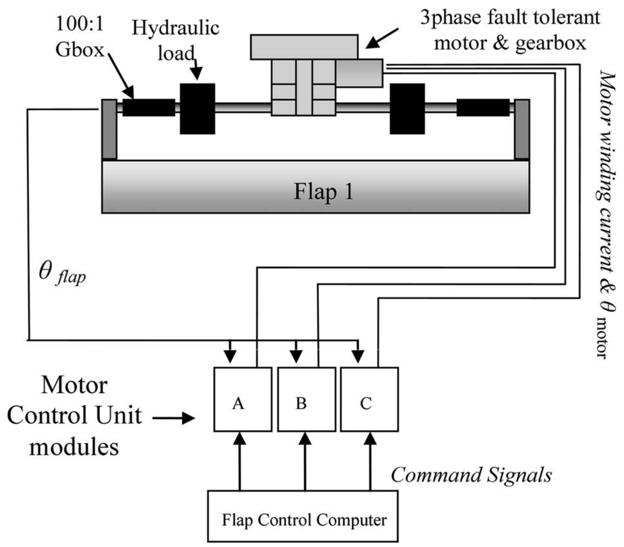


Fig. 2. Overview of a flap drive.

addition to the resolver motor position sensors used to control the motor currents. The flap position is determined by cross-correlating the data from the linear position sensors. The flap control computer receives supervisory data from the three drive modules and sets speed and torque demand limits for the modules. However, the flap control computer does not close the position loop; this is done in the drive modules. The drive modules also cross-communicate status information.

Wing surface loading is achieved using a large hydraulic load rig, which can exert full-load torque, profiled to represent the variation of load with position.

The second half-flap is included to demonstrate symmetry between surfaces. The flap surface and linkage arms are only simplified visual indicators of movement.

## II. Drive Specification and Architecture

An electric actuator consisting of an electric motor, providing 3.4 Nm of torque at up to 10 000 r/min (i.e., 3.5 kW), with an integral power-off friction brake and a dual step-down gearbox has been designed and built. The maximum load on the flap is 34 kN · m, but this is through both the gearbox in the flap mechanism and the new actuator gearbox, so the combined step-down ratio is on the order of 10 000 : 1.

Earlier research has demonstrated that the greatest torque density can be achieved with a permanent-magnet machine [12], and fault-tolerant permanent topologies have been developed and extensively tested. For these reasons, a permanent-magnet brushless drive has also been selected for this application.

The strategy adopted for fault-tolerant drives has been to split the drive into a series of smaller modules, each of which is independent of all others [13]–[20]. To prevent common-mode failures, there are separate controllers, power electronic converters, and position sensors for each module.

The motor is best thought of as a series of separate independent motors in a single casing. Although these motors share the same rotor and stator laminations, each one is magnetically, thermally, and mechanically independent of all others. The only modes of common failure that could occur are mechanical, due to bearing failure or mechanical failure of the rotor assembly. Based on the experience of industrial authors, when good maintenance strategies are employed, mechanical failures are reduced to acceptable levels.

When designing the drive, it is necessary to balance drive mass and volume against increased complexity. Two topologies were considered: one in which the overall drive is made from a series of single-phase units and one in which it is constructed from a series of three-phase units.

Research has shown that critical sizing requirements resulted from three operating conditions [7], [8], which must be met, even when there has been a failure.

1) *At standstill*, the motor needs to provide full torque at all rotor angles in order to start rotation. If there is loss of torque from one module, then the shortfall must be made up by the remaining healthy modules. Multiple three-phase modules each can produce full torque at all rotor positions, so there is simply a scaling of the torque. For a drive consisting of single-phase modules, it is necessary to reshape the current in the remaining phase modules to produce full torque [8], [19], [20].
2) *At low speed*, if a phase is short-circuited, then it will induce a drag torque of up to half the original motoring torque. Clearly, the more phases (or sets of three phases) a motor consists of, the lesser the overall effect that this drag torque exerts.
3) *At high speed,* the functioning proportion of the motor must account for the drop in mean torque due to a failed phase.

Detailed evaluation of these three conditions [7] has shown that the best compromise between size and complexity occurs when the drive consists of three independent single-phase modules. This configuration has been selected, with each phase module driven by a single-phase voltage-fed inverter. It should be noted that the maximum power consumed when the machine is faulted is hardly any greater than when it is fully healthy, because maximum power occurs near the highest speed when the drag torque from the faulted phase is very small.

## III. Prototype Construction

Fig. 3 shows the gearbox driven from a single motor. A junction box on the gearbox gives a visual representation of the housing for the drive electronics.

### A. Controller Architecture

Each motor phase requires a completely isolated electric drive for control: a triplex control architecture provides a good compromise between reliability and complexity. Fig. 4 shows the triplex control architecture of the actuator.

Each drive module cross-compares data with other modules at an iteration rate of 100 Hz. Input data from the Flap Control Computer are cross-compared, and a median value is selected, so any of the three lanes can operate with a failed command input lane. Input data from transducers on the flap, the three

Authorized licensed use limited to: Newcastle University. Downloaded on May 21,2010 at 13:17:05 UTC from IEEE Xplore. Restrictions apply.

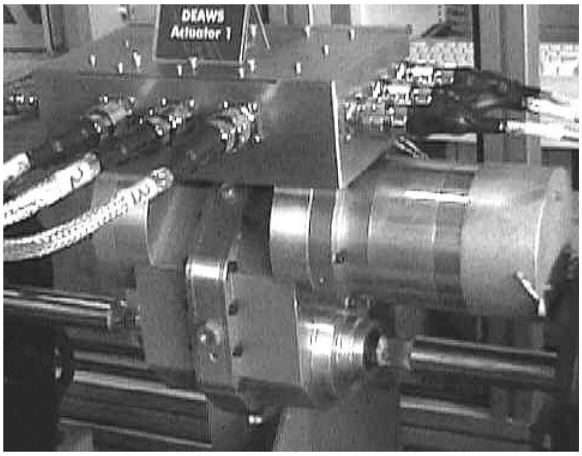


Fig. 3. Motor and gearbox.

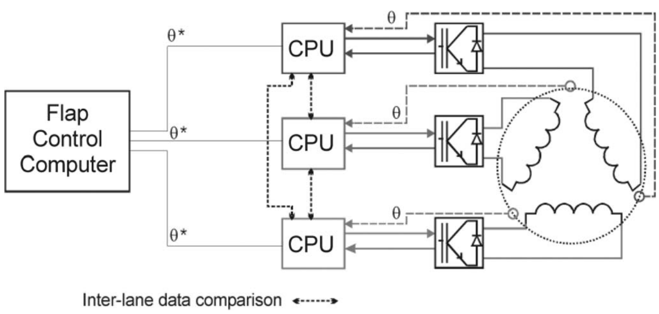


Fig. 4. Triplex control architecture.

motor resolvers, and a transducer inside the gearbox are also cross-compared.

The control scheme uses the consolidated position demand from the flap control computer with position feedback from linear position transducers on the flap tracks to provide a torque demand on a 100-Hz iteration rate in each drive. Inner current loops operate at 10 kHz. Once the demanded position has been attained, the friction brakes are applied to the motor, and the current is set to zero to avoid driving against the brakes. The friction brakes require 24 Vdc to release and have dual electromagnetic caliper windings, each capable of releasing the brake. A brake driver module for each winding cross-compares release votes from the drive lanes.

As it is crucial that surfaces remain symmetrical, dynamic speed-limiting ensures that all actuators run at the rate of the slowest surface. It is also possible for the Flap Control Computer to disable any lane, or even two, causing the friction brakes to automatically operate.

For ease of development, the electric drive uses a single digital signal processing (DSP) unit and field-programmable gate array module to control three power electronic converters. The triplex control architecture is internally simulated in software with three RS-232 interfaces connecting the DSP to a flap control computer emulator.

### B. Rotor Angle Sensing

Sensorless operation is possible [21], but, in this case, redundancy is simply incorporated into the rotor-position-sensing

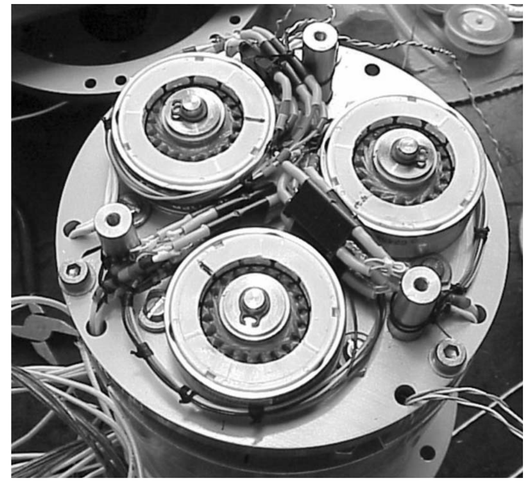

Fig. 5. One end of the electrical machine, showing the three resolvers.

hardware. To prevent any common modes of failure, a separate resolver is used for each phase module, as shown in Fig. 5. In this case, the three resolvers are coupled to the shaft via a gear system, with each resolver containing a locating pin that will shear in the event of the resolver locking. This arrangement ensures that the failure of one resolver does not affect the operation of the other two.

## IV. Operation of Full Demonstrator Rig

### A. General

The full rig has been subjected to extensive testing, including the following aspects:

1) machine electromagnetic performance;
2) drive thermal performance;
3) synchronization between adjacent flaps driven by separate drives;
4) low-speed operation with one phase disabled;
5) high-speed operation with one phase disabled;
6) operation with a failed resolver;
7) operation with disabled communications links.

This section will initially outline the test conditions employed before illustrating the measured drive performance in the unfaulted condition. Faulted operation at low speed will then be demonstrated, illustrating how the drive reshapes the healthy phase currents in order to produce full measured torque at all rotor positions. There will then be consideration of flap–flap synchronization and thermal performance.

### B. Test Conditions

Fig. 6 shows a worst case profile (in terms of the demands placed on the actuator) of extensions and retraction, with a 1-min rest period repeatedly performed on both flap systems. This corresponds to the training condition when the aircraft is repeatedly taking off and landing. In addition, during the testing described later in this paper, a fault condition was imposed on phase 1 of the second actuator, so that full torque had to be generated from the remaining two phases.

Authorized licensed use limited to: Newcastle University. Downloaded on May 21,2010 at 13:17:05 UTC from IEEE Xplore. Restrictions apply.

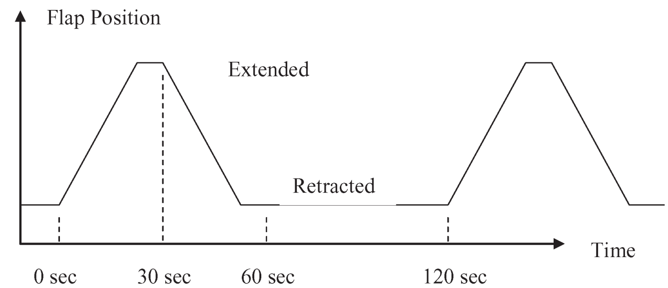


Fig. 6. Load profile for worst case continuous testing.

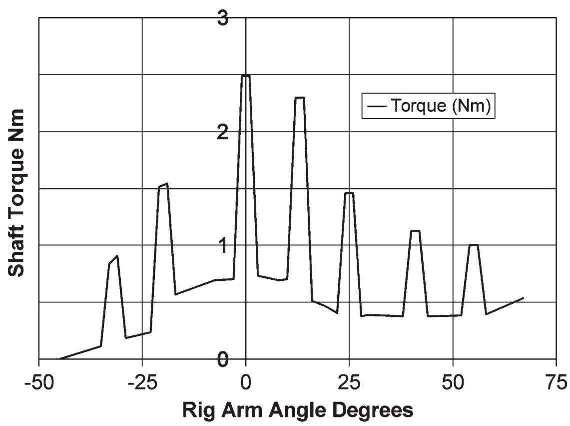


Fig. 7. Motor torque and flap arm angles under worst case load profile + sporadic spoiler extensions.

Fig. 7 shows the motor torque requirement of a single flap when the worst load profile condition is applied over one extension. The basic pattern of torque comes from the aerodynamic load and the mechanics of the actuation mechanism. It reaches a maximum partway through the extension. The load torque shown in Fig. 7 has also had, superimposed on it, seven short periods, where the torque is increased by a factor of 3.5 to represent the extra aerodynamic loads created by spoiler extensions (such as might happen during a landing, with the spoilers being repeatedly deployed to slow the aircraft down as the flaps are being extended).

### C. Low-Speed Operation Unfaulted

Fig. 8 shows the measured three-phase current waveforms in a single actuator as it starts up, producing rated torque. This requires peak instantaneous phase currents of approximately 20 A. The actuator is initially held in position by the electric brake, and the motor must be powered before the brake is released to prevent runaway. Consequently, for the first 12 ms of the test, the actuator is stationary, and initial dc currents occur. Once running, the phase currents are essentially sinusoidal.

### D. Low-Speed Operation Faulted

Fig. 9 shows the measured operation of the drive when a phase is shut down midoperation, simulating a single-phase fault. For this particular test case, the drive is running at 3000 r/min. The remaining healthy phases must compensate for the faulted phase, so that the mean output torque of the drive is unaltered when operating at high speed. At low speed, the

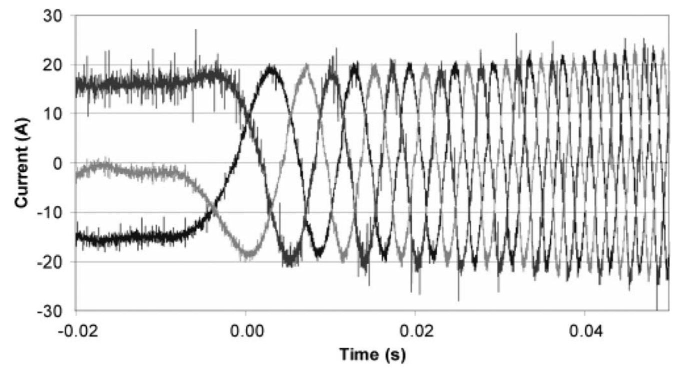


Fig. 8. Startup currents after brake is released.

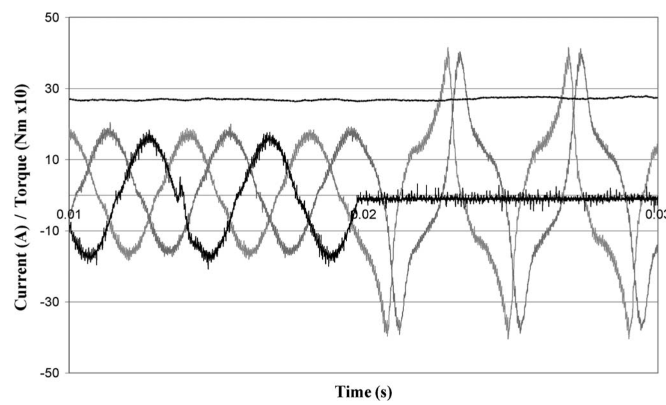


Fig. 9. Measured motor phase currents and sum output torque after phase shutdown. The top line is the sum torque.

requirements are more stringent; the inertia of the drive may not be enough to carry through any torque dips, and consequently, the drive must continue to produce rated torque at all rotor positions.

The drive controller operates as described here.

1) A fault is detected, and its cause is identified by the controller. The fault can be in the machine, the power electronics, or the controller. Cross-comparison between phase controllers plays a strong role in this process.
2) Once the fault is identified, actions are taken in the hardware to limit the fault current to within rated values, thereby preventing overheating and fault propagation. For the example shown in Fig. 9, an open-circuit failure is imposed, so the currents in the faulted phase are zero, giving a relatively benign condition.
3) For most fault conditions, there is no longer full control of the current in the faulted phase. The controller then monitors the faulted phase current and hence deduces its instantaneous torque contribution in real time. This is subtracted from the drive torque demand to produce an instantaneous torque requirement for the remaining two healthy phases.
4) The torque requirement for the two healthy phases is apportioned between each phase according to its instantaneous torque constant. Real-time instantaneous per-phase currents are then deduced using the torque constants. This method can be shown to give the minimum rms drive phase current and, hence, minimum winding loss

Authorized licensed use limited to: Newcastle University. Downloaded on May 21,2010 at 13:17:05 UTC from IEEE Xplore. Restrictions apply.

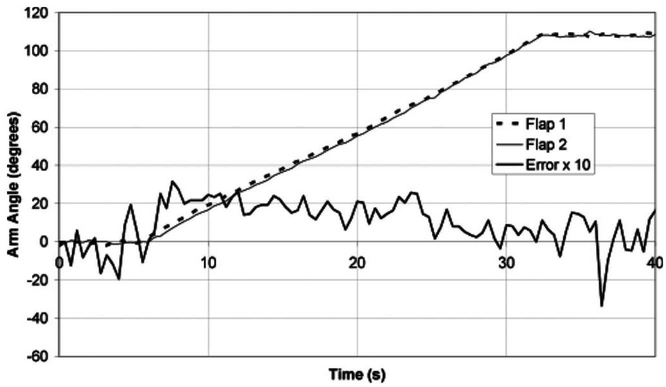


Fig. 10. Synchronization of two flaps during extension.

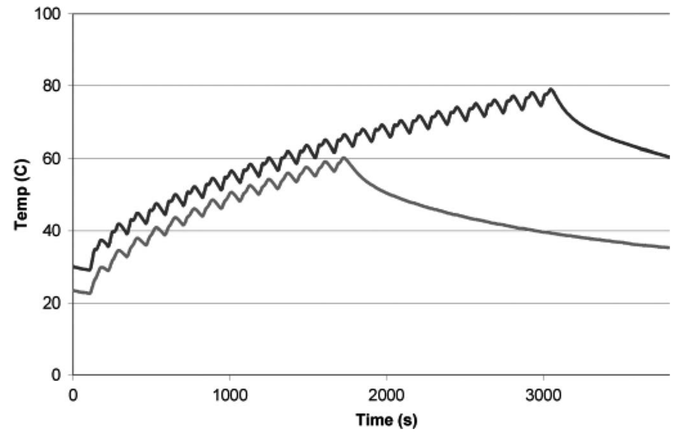


Fig. 11. Thermal performance of two actuators (higher trace running faulted).

[7]. Unless further modifications are made, it does not, however, minimize the peak phase currents.

5) The waveforms in Fig. 9 show the process in action in the drive. At a time of 0.02 s, one phase has an open-circuit fault and can no longer contribute to torque. The current waveforms of the remaining two phases are boosted in certain parts of their cycle to produce a rather unusual wave shape. Note that the periods of peak current coincide with the times when the faulted phase would make a major contribution to torque, and so, the healthy currents have to be boosted by almost a factor of two. The shaft torque for this test has been measured with a high-bandwidth torque transducer and is also shown in Fig. 9. The shaft torque remains unaltered by the occurrence of the fault.

### E. Flap Synchronization

Fig. 10 shows the measured positions of two adjacent flaps during flap extensions on the test rig. There is a requirement for the two flaps to be closely synchronized at all times, and so, the drives for each flap must precisely be coordinated during their movement. The torque demand upon each flap varies according to its position on the wing, and this is also included in the model, so the two flaps have differing loads.

To give a worst case condition, a fault has been imposed on one phase of flap 2's actuator. Fig. 10 shows the degree to which the two flaps remain synchronized. Remembering the specification that was for $+/-0.25\%$ of full-scale deflection when retracted (i.e., close to $+/-0.25^\circ$ in this case, as full scale is $112^\circ$) and $+/-0.5\%$ at other positions, it can be seen that, at certain angles, the error in the demonstrator is many times the allowable limit. More than half of the error is actually due to backlash in the demonstrator output gearbox; with an operational output gearbox, the actuator will already meet the specification. Of the rest of the error, some is due to imperfect tuning, and the most of the rest relates to the accuracy of the position feedback. It will be possible to get synchronization accuracy well within the tolerance.

### F. Thermal Performance

Fig. 11 shows the temperature measured at the center of a winding (which is the location of the hot spot in the machine) of two actuators driving adjacent flaps with the load profile of Fig. 7 continuously applied. The lower curve is with no faults, whereas the upper curve is running on two phases. The lower actuator is switched off after 1800 s to demonstrate cooling behavior. Fitting exponentials to the measured faulted curve reveals a maximum steady-state temperature of 91 °C against an ambient of 30 °C, i.e., a rise of 61 °C. Taking a maximum ambient of 70 °C would give a maximum temperature of 131 °C, which is well within the limits for the winding of about 160 °C.

## V. Conclusion

A full-scale demonstrator of a distributed electrical aircraft flap system has been built and tested. The system contains two fault-tolerant electric drives and associated gearboxes driving against loads typical of a flap system, produced using hydraulic loads to meet safety requirements.

The system is able to meet its specification, including synchronization between adjacent flaps and operation in the event of a machine or controller failure. Results have demonstrated operation with a single-phase open-circuit failure. The system detects the failure and modifies the remaining healthy phases in order to continue to produce smooth torque at all rotor positions. It is shown that the shaft torque remains essentially unchanged by the fault.

## Acknowledgment

The authors would like to thank Comar Engineering Ltd. for the design and construction of the load rig.

## References

[1] D. T. Glass-Hooper, "The electric control of large aeroplanes," *Flight*, p. 1118, Dec. 21, 1916.
[2] J. Rea, "Boeing 777 high lift control system," *IEEE Aerosp. Electron. Syst. Mag.*, vol. 8, no. 8, pp. 15–21, Aug. 1991.
[3] S. C. Jensen, G. D. Jenny, and D. Dawson, "Flight test experience with an electromechanical actuator on the F-18 systems research aircraft," in *Proc. 19th DASC*, Oct. 2000, vol. 1, pp. 2E3/1–2E3/10.
[4] K. C. Thompson, K. Eitenmiller, and C. L. Hunter, "Demonstration of electric actuator technology for military transport aircraft," in *Proc. NAECON*, May 1983, p. 87.
[5] K. C. Thompson and R. E. Alden, "Lockheed-Georgia and electric primary flight control systems," in *Proc. NAECON*, May 1985, p. 588.

Authorized licensed use limited to: Newcastle University. Downloaded on May 21,2010 at 13:17:05 UTC from IEEE Xplore. Restrictions apply.

[6] D. E. Blanding, "An assessment of the developing dual use electric actuation technologies for military aircraft and commercial application," in *Proc. 32nd IECEC*, Jul./Aug. 1997, vol. 1, pp. 716–172.
[7] J. W. Bennett, B. C. Mecrow, A. G. Jack, D. J. Atkinson, C. Sewell, G. Mason, S. Sheldon, and B. Cooper, "Choice of drive topologies for electrical actuation of aircraft flaps and slats," in *Proc. IEE Conf. Power Electron., Mach. Drives*, Edinburgh, U.K., Mar. 2004, pp. 332–337.
[8] J. W. Bennett, A. G. Jack, B. C. Mecrow, D. J. Atkinson, C. Sewell, and G. Mason, "Fault tolerant control architectures for an electrical actuator," in *Proc. IEEE PESC*, Aachen, Germany, 2004, pp. 4371–4377.
[9] *IEEE Recommended Practice for Reliable Industrial and Commercial Power Systems*, IEEE Gold Book, 2007, pp. 213–303.
[10] P. J. Tavner and J. P. Hasson, "Predicting the design life of high integrity rotating electrical machines," in *Proc. IEE 9th EMD*, Canterbury, U.K., Sep. 1–3, 1999, pp. 286–290.
[11] B. C. Mecrow, A. J. Atkinson, A. G. Jack, S. Green, J. A. Haylock, and J. Coles, "The need for fault tolerance in an aeroengine electric fuel control system," in *Proc. IEE Colloq. Elect. Mach. Syst. More Elect. Aircraft*, London, U.K., Nov. 9, 1999, pp. 9/1–9/5.
[12] A. G. Jack, B. C. Mecrow, and J. Haylock, "A comparative study of permanent magnet and switched reluctance motors for high performance fault tolerant applications," *IEEE Trans. Ind. Appl.*, vol. 32, no. 4, pp. 889–895, Jul./Aug. 1996.
[13] T. M. Jahns, "Improved reliability in solid state A.C. drives by means of multiple independent phase-drive units," *IEEE Trans. Ind. Appl.*, vol. 16, no. 3, pp. 321–331, May 1980.
[14] B. C. Mecrow, A. G. Jack, and J. A. Haylock, "Fault tolerant permanent magnet machine drives," *Proc. Inst. Elect. Eng.*, vol. 143, no. 6, pt. B, pp. 437–442, Nov. 1996.
[15] E. Richter, "Switched reluctance machines for high performance operations in a harsh environment—A review paper," in *Proc. ICEM Conf.*, Boston, MA, 1990, pp. 18–24.
[16] T. J. E. Miller, "Faults and unbalanced forces in the switched reluctance machine," *IEEE Trans. Ind. Appl.*, vol. 31, no. 2, pp. 319–328, Mar./Apr. 1995.
[17] J. A. Haylock, B. C. Mecrow, A. G. Jack, and D. J. Atkinson, "On-line detection of winding short-circuits in inverter fed drives," in *Proc. 9th EMD*, Canterbury, U.K., Sep. 1–3, 1999, pp. 258–262.
[18] T. Gopalarathnam, H. A. Toliyat, and J. C. Moreira, "Multi-phase fault-tolerant brushless DC motor drives," in *Conf. Rec. IEEE IAS Annu. Meeting*, Oct. 8–12, 2000, vol. 3, pp. 1683–1688.
[19] A. G. Jack and B. C. Mecrow, "Safety critical drives for aerospace applications," in *Proc. ICEM*, Paris, France, Sep. 1994, pp. 91–96.
[20] D. Ede, K. Atalah, J. B. Wang, and D. Howe, "Modular fault-tolerant permanent magnet brushless machines," in *Proc. Int. Conf. Power Electron., Mach. Drives*, Apr. 16–18, 2002, pp. 415–426.
[21] S. Green, D. J. Atkinson, A. G. Jack, B. C. Mecrow, and A. King, "Sensorless operation of a fault tolerant PM drive," *Proc. Inst. Elect. Eng.—Elect. Power Appl.*, vol. 150, no. 2, pp. 117–125, Mar. 2003.

**John W. Bennett** received the M.Eng. degree in electrical and electronic engineering from the University of Newcastle upon Tyne, Newcastle upon Tyne, U.K., in 2001. He is currently working toward the Ph.D. degree in fault-tolerant electric actuators in the Department of Electrical, Electronic and Computer Engineering, University of Newcastle upon Tyne.

In 2001, he became a Research Associate at the University of Newcastle upon Tyne and has developed power electronic drives for a number of university and industrial research projects, including propulsion for unmanned aerial vehicles and fault-tolerant actuators for aircraft flaps and nose-wheel steering.

**Barrie C. Mecrow** (M'98) received the Ph.D. degree from the University of Newcastle upon Tyne, Newcastle upon Tyne, U.K., for his research into 3-D eddy-current computation applied to turbogenerators.

He worked as a Turbogenerator Design Engineer with NEI Parsons, U.K. In 1987, he became a Lecturer at the University of Newcastle upon Tyne, Newcastle upon Tyne, U.K., and is currently a Professor of electrical power engineering in the Department of Electrical, Electronic and Computer Engineering. His research interests are fault-tolerant drives, high-performance PM machines, and novel switched reluctance drives.

**Alan G. Jack** (M'00) received the Ph.D. degree from Southampton University, Southampton, U.K., in 1975, for his work on numerical analysis of electromagnetic fields in turbogenerators.

He has been the Department's Chair in electrical engineering, a past Department Head, and the leader of the Newcastle Electric Drives and Machines Group. He has been with the University of Newcastle upon Tyne, Newcastle upon Tyne, U.K., for more than 20 years, joining them from NEI Parsons, with whom he spent 13 years, with roles ranging from Craft Apprentice to Principal Design Engineer. He is currently with the Department of Electrical, Electronic and Computer Engineering, University of Newcastle upon Tyne. He is the author of more than 80 papers in the area of electrical machines and drives.

**David J. Atkinson** received the Ph.D. degree from the University of Newcastle upon Tyne, Newcastle upon Tyne, U.K., for his research into the use of Kalman-filter-based estimation on induction motor vector-controlled drives.

He is currently a Senior Lecturer in the Drives and Machines Group, Department of Electrical, Electronic and Computer Engineering, University of Newcastle upon Tyne. Prior to his university appointment in 1987, he had spent 17 years in industry. His research interests include electrical drive systems, real-time estimation and control, power electronics, and wind power generation. His current research interests include sensorless vector drives, fault-tolerant drives, and cascade induction generators.

Authorized licensed use limited to: Newcastle University. Downloaded on May 21,2010 at 13:17:05 UTC from IEEE Xplore. Restrictions apply.